ACS OMEGA

Article

Cite This: ACS Omega 2019, 4, 6264−6272

http://pubs.acs.org/journal/acsodf

Simultaneous Prediction of Cosolvent Influence on Reaction Equilibrium and Michaelis Constants of Enzyme-Catalyzed Ketone Reductions

Anton Wangler, Aline Hüser, Gabriele Sadowski, and Christoph Held*

Laboratory of Thermodynamics, Department of Biochemical and Chemical Engineering, TU Dortmund University, Emil-Figge-Str. 70, 44227 Dortmund, Germany

Supporting Information

ABSTRACT: Understanding and quantification of cosolvent influences on enzyme-catalyzed reactions are driven by a twofold interest. On the one hand, cosolvents can simulate the cellular environment for deeper understanding of in cellulo reaction conditions. On the other hand, cosolvents are applied in biotechnology to tune yield and kinetics of reactions. Further, cosolvents are even present inherently, for example, for reactions with cofactor regeneration or for enzymes that need cosolvents in a function of a stabilizer. As the experimental determination of yield and kinetics is costly and time consuming, this work aims at providing a thermodynamic predictive approach that might allow screening cosolvent influences on yield and Michaelis constants. Reactions investigated in this work are the reduction of butanone and 2-pentanone under the influence of 17 wt % of the cosolvent polyethylene glycol 6000, which is also often used as a crowder to simulate cellular environments. The considered reactions were catalyzed by a genetically modified alcohol dehydrogenase (ADH 270). Predictions of cosolvent influences are based on accounting for a cosolvent-induced change of molecular interactions among the reacting agents as well as between the reacting agents and the solvent. Such interactions were characterized by activity coefficients of the reacting agents that were predicted by means of electrolyte perturbed-chain statistical associating fluid theory. This allowed simultaneously predicting the cosolvent effects on yield and Michaelis constants for two-substrate reactions for the first time.

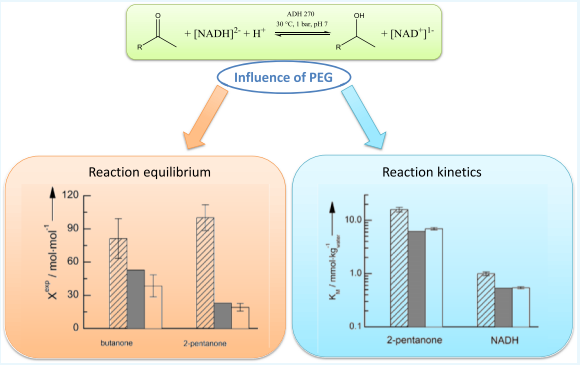

INTRODUCTION

Biocatalytic processes are rising within the chemical industry as they often present meaningful alternatives to chemically catalyzed routes. New developments in enzyme design and a deeper understanding into biocatalysis lead to highly suitable catalysts for the production of fine chemicals[1] and for a wider range of applications.[2] Enzymes enable reaction catalysis under mild conditions (often ambient pressure and temperature), while providing high selectivity toward one product often with high enantioselectivity.[3,4] Further, the application of enzymes can turn environmentally hazardous reactions requiring strong acids or toxic solvents into "green" reactions, minimizing waste, and emissions.[5,6]

Enzyme-catalyzed reactions are characterized by the key properties reaction equilibrium and reaction rate, and the latter contains kinetic parameters such as Michaelis constants.[7,8] The Michaelis constant is an indicator for the cellular concentration range of a substrate as any increase of the substrate's concentration above the value of the Michaelis constant will maximally double the reaction rate. Thus, (micro-)organisms use substrate concentrations often not much higher than the value for the Michaelis constant.[8,9] While the reaction equilibrium is known to be independent of the catalyst as long as the catalyst is present at low concentration,[10−14] the reaction rate and Michaelis constants strongly depend on the catalyst.[15,16] Further, both, reaction equilibrium and Michaelis constants strongly depend on the reaction medium, which might be tuned by the addition of cosolvents. This influence of cosolvents is often described empirically based on experimental data, which is costly and time consuming. Thus, it is desired to predict the cosolvent influence on reaction equilibrium and on Michaelis constants without the requirement of experimental data concerning the reactive system containing cosolvents. Such predictions are important for the design and improvement of biochemical reactions. Further, the ability to quantitatively predict such behavior enables a deeper understanding of the reason behind the cosolvent influence on reaction equilibrium and Michaelis constants. Especially, the interaction between cosolvent and the active site(s) of an enzyme is studied in the literature; commonly, this is done at an atomistic level using molecular dynamics simulation for the direct interaction between solvent molecules and single amino

Received: November 13, 2018
Accepted: January 18, 2019
Published: April 4, 2019

DOI: 10.1021/acsomega.8b03159
ACS Omega 2019, 4, 6264−6272

acids of the enzyme's active site.[17−19] While these studies try to get access to molecular interactions on the single atom level, previous works from the literature[20,21] and by our group[10,11,13−16,22] have shown that these detailed studies might not be required to predict cosolvent influences on the reaction equilibrium and Michaelis constants of enzyme-catalyzed reactions. Thus, cosolvent−enzyme interactions are not decisive given that the cosolvent does neither denature the enzyme nor acts as a substrate/inhibitor.

That is, predictions of cosolvent influences on reaction equilibrium and Michaelis constants of reactions are based on understanding and quantification of molecular interactions among the reacting agents and between the reacting agents and the solvent (cosolvent) in the reaction mixture. For this purpose, changes of the chemical potential are quantified in form of activity coefficients of the reacting agents in the presence of the cosolvent. The most prominent models proposed for the prediction of these molecular interactions are the electrolyte nonrandom two-liquid model,[23] the Debye−Hückel extended UNIQUAC equation,[24] the Pitzer model,[25] the conductor-like screening model,[26] or the electrolyte perturbed-chain statistical associating fluid theory (ePC-SAFT) equation of state.[27] As was shown by Grosch,[21] Pleiss,[20] and previous work,[11,15,16] these models are capable to predict cosolvent influences on activity coefficients of reacting agents properly. In this work, ePC-SAFT is used for this purpose for several reasons: first, the reacting agents are charged species which requires an electrolyte model; second, polymers are considered as cosolvents in this work, and classical PC-SAFT is especially suitable for polymer/solvent systems;[28] third, ePC-SAFT has shown to be able to predict activity coefficients in electrolyte systems consisting of multiple components in previous works.[10,13,14,22,29,30]

The reactions studied in this work are the reduction of butanone and the reduction of 2-pentanone, catalyzed by a genetically modified alcohol dehydrogenase (ADH 270) with the required cofactor NADH + H^+ at pH 7, 30 °C, and 1 bar. The reaction mechanism of such ketone reductions is shown in Figure 1. Please note that the true reacting species $[NADH]^{2-}$ will be referred to as NADH, and $[NAD^+]^-$ will be referred to as NAD^+ according to recommendations,[31] previous work,[10,13] and textbook knowledge.[32]

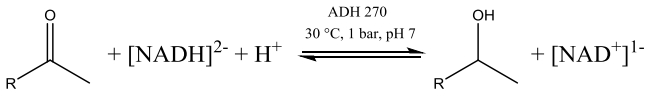

Figure 1. Reaction scheme of the reduction of a ketone (in this work: butanone and 2-pentanone) to the respective alcohol (in this work: butanol and 2-pentanol) with the cofactor nicotinamide adenine dinucleotide in its protonated form (NADH + H^+) and deprotonated form (NAD^+) catalyzed by a genetically modified alcohol dehydrogenase (ADH 270) in aqueous medium.

In this work, the reduction of the substrates butanone and 2-pentanone were investigated because of previous work on the aromatic ketone acetophenone and the successful predictions of the reaction equilibrium[10] and the Michaelis constants[15,16] under cosolvent influence. The cosolvent regarded in this work is polyethylene glycol 6000 (PEG 6000) with a concentration of 17 wt %. PEG was used in this work, as it is chemically inert, and thus, it is not involved in the reaction as a reacting participant. Although PEG is often applied in similar concentration ranges as an enhancer for reactions[33−36] or as a phase former for aqueous two-phase systems which is required for in situ product removal,[37−42] PEG is also suitable as a crowder molecule for the study of reactions on a more cellular level.[43,44]

The approach presented in this work might be used as a screening tool for the influence of cosolvents on reaction equilibrium and Michaelis constants of many other enzyme-catalyzed reactions. This allows more efficient process design in future and a better understanding of reactions under in cellulo conditions.

THEORETICAL FRAMEWORK

Reaction Equilibrium. The thermodynamic equilibrium constant K_{th} for the reduction of butanone and 2-pentanone can be determined according to eq 1.

$$K_{th} = K_x^{obs} \cdot K_\gamma' = \frac{x_{alcohol} \cdot x_{NAD^+}}{x_{ketone} \cdot x_{NADH}} \cdot \frac{\gamma_{alcohol} \cdot \gamma_{NAD^+}}{\gamma_{ketone} \cdot \gamma_{NADH}} \cdot \frac{1}{a_{H^+}} \quad (1)$$

In this work, species-averaged activity coefficients of NAD^+ and NADH were used to reduce the complexity of the system without sacrificing the quality of the predictions as shown in previous works and thus K_{th} reference to the biochemical reference state commonly indicated by K'_{th}.[10,15,16] As K_x^{obs} (the ratio of the mole fractions of the reacting agents at equilibrium) strongly depends on kind and concentration of the cosolvent, it is further referred to as an observed (obs) value; thus, it is *not* a constant value. In contrast to eq 1, the activity of H^+ is transferred to the side of K_{th} in eq 2.

$$K_{th} \cdot a_{H^+} = X^{obs} \cdot \Gamma = \frac{x_{alcohol} \cdot x_{NAD^+}}{x_{ketone} \cdot x_{NADH}} \cdot \frac{\gamma_{alcohol} \cdot \gamma_{NAD^+}}{\gamma_{ketone} \cdot \gamma_{NADH}} \quad (2)$$

$$X^{obs} = \frac{x_{alcohol} \cdot x_{NAD^+}}{x_{ketone} \cdot x_{NADH}} \quad (3)$$

$$\Gamma = \frac{\gamma_{alcohol} \cdot \gamma_{NAD^+}}{\gamma_{ketone} \cdot \gamma_{NADH}} \quad (4)$$

This was done as the pH was kept constant by the use of a 4-(2-hydroxyethyl)-1-piperazineethanesulfonic acid (HEPES) buffer, and thus, the activity of H^+ was constant in this work, which leads to a constant value for $K_{th} \cdot a_{H^+}$. Although H^+ is a reacting agent, the H^+-free mole-fraction ratio X^{obs} is a more suitable indicator for the equilibrium position, and thus, X^{obs} is further used instead of K_x^{obs}.

Measuring X^{obs} for the neat (cosolvent free) conditions and having access to Γ by means of ePC-SAFT predicted activity coefficients allows determining the cosolvent independent value $K_{th} \cdot a_{H^+}$. On the basis of this constant value (at constant temperature and pH), the influence of cosolvents is expressed in Γ, which then allows predicting X^{pre}. This prediction is based on minimizing the objective function OF1 as shown in eq 5 iteratively. A scheme of the iteration process including input parameters and the iteration loop is given in the Supporting Information.

$$OF1: \left| \frac{K_{th}(neat) - L}{K_{th}(neat)} \right| \leq 10^{-5} \quad (5)$$

$$L = \frac{x_{alcohol} \cdot x_{NAD^+}}{x_{ketone} \cdot x_{NADH}} \cdot \frac{\gamma_{alcohol} \cdot \gamma_{NAD^+}}{\gamma_{ketone} \cdot \gamma_{NADH}} \quad (6)$$

DOI: 10.1021/acsomega.8b03159
ACS Omega 2019, 4, 6264−6272

Table 1. Overview about the ePC-SAFT Pure-Component Parameters Used in This Work[a]

component	m_i^{seg} [−]	σ_i [Å]	u_i/k_B [K]	N_i^{assoc}	$\varepsilon^{A_iB_i}/k_B$ [K]	$\kappa^{A_iB_i}$ [−]
water[52]	1.204	[b]	353.95	1:1	2425.7	0.0451
NADH[10]	27.27	2.22	260.72	8:8	3581.9	0.001
NAD^+[10]	24.93	2.23	299.04	8:8	3557.3	0.001
PEG[41]	M_{PEG}·0.050	2.90	204.60	4:4	1799.8	0.020
butanone[53]	3.074	3.39	252.27			
2-butanol[54]	3.440	3.31	224.20	1:1	2067.6	0.0104
2-pentanone[53]	3.430	3.47	249.83			
2-pentanol[55]	2.782	3.80	260.16	1:1	2697.81	0.0065
Na^+[56]	1	2.82	230.0			
OH^-[56]	1	2.02	650.0			

[a]These include the segment number m_i^{seg}, segment diameter σ_i, dispersion energy parameter u_i/k_B, association scheme N_i^{assoc}, association energy parameter $\varepsilon^{A_iB_i}/k_B$, and association volume parameter $\kappa^{A_iB_i}$. [b]$k_{ij}(T) = -0.135 + 0.0023439\cdot(T[K] - 298.15)$.

Reaction Kinetics. The Michaelis–Menten equation for a two-substrate reaction is expressed with eq 7 as proposed in the literature.[7,8]

$$\frac{1}{\nu'} = \frac{m_E}{\nu} = \left(\frac{K_{i,NADH}^{obs}\cdot K_{M,ketone}^{obs}}{k_{cat}\cdot m_{ketone}} + \frac{K_{M,NADH}^{obs}}{k_{cat}}\right)\cdot\frac{1}{m_{NADH}} + \left(\frac{K_{M,ketone}^{obs}}{k_{cat}\cdot m_{ketone}} + \frac{1}{k_{cat}}\right) \quad (7)$$

K_M strongly depends on kind and concentration of cosolvent; thus, the measured value for K_M is denoted as the observed value K_M^{obs} in the following. In eq 7, ν' is the reaction rate normalized to the total enzyme concentration m_E; this is required to make experiments with different enzyme concentrations comparable to each other. Further, $K_{M,ketone}^{obs}$ and $K_{M,NADH}^{obs}$ represent the Michaelis constants of the ketone (butanone; 2-pentanone) and NADH, respectively. The highest achievable normalized reaction rate is given by k_{cat}, while m_{ketone} and m_{NADH} denote the initial molalities of the respective ketone substrate (butanone; 2-pentanone) and NADH. $K_{i,NADH}^{obs}$ represents the inhibition constant of NADH toward the ketone substrate; combined with $K_{M,NADH}^{obs}$ the exact value of the inhibition constant is required to define the reaction mechanism. If $K_{i,NADH}^{obs}$ proves to be equal to $K_{M,NADH}^{obs}$ a random binding mechanism is prevailing, while a ping-pong mechanism is present if $K_{i,NADH}^{obs} = 0$. Otherwise, an ordered binding mechanism is given in which NADH (or the ketone) binds first if $K_{i,NADH}^{obs} < K_{M,NADH}^{obs}$ (or if $K_{i,NADH}^{obs} > K_{M,NADH}^{obs}$).[7,45] To determine all the kinetic properties $K_{M,ketone}^{obs}$, $K_{M,NADH}^{obs}$, k_{cat}, and $K_{i,NADH}^{obs}$, a two-step linearization was applied in this work. A detailed description of the two-step linearization is given in the Supporting Information. To convert $K_{M,ketone}^{obs}$ and $K_{M,NADH}^{obs}$ to their activity-based Michaelis constants $K_{M,ketone}^{a}$ and $K_{M,NADH}^{a}$, molalities in eq 7 were replaced by thermodynamic activities $a = m_i\cdot\gamma_i^m$, leading to eq 8

$$\frac{1}{\nu'} = \left(\frac{K_{i,NADH}^{a}\cdot K_{M,ketone}^{a}}{k_{cat}\cdot a_{ketone}} + \frac{K_{M,NADH}^{a}}{k_{cat}}\right)\cdot\frac{1}{a_{NADH}} + \left(\frac{K_{M,ketone}^{a}}{k_{cat}\cdot a_{ketone}} + \frac{1}{k_{cat}}\right) \quad (8)$$

The big advantage of $K_{M,ketone}^{a}$ and $K_{M,NADH}^{a}$ over their molality-based pendants is that $K_{M,ketone}^{a}$ and $K_{M,NADH}^{a}$ are independent of any cosolvent. It was shown in our own previous works[15,16] and in other literature[20,21,46] that converting molalities to thermodynamic activities does still preserve information on the reaction mechanism; thus, the assumptions needed to derive eq 7 as given in the literature[7,8] are not violated. $K_{M,ketone}^{a}$ and $K_{M,NADH}^{a}$ were determined in analogy to $K_{M,ketone}^{obs}$ and $K_{M,NADH}^{obs}$ through the two-step linearization presented. The ePC-SAFT predictions of $K_{M,ketone}^{obs}$ and $K_{M,NADH}^{obs}$ under cosolvent influence are described in detail in the Supporting Information.

As predictions for X^{obs} and K_M^{obs} under cosolvent influence require the respective activity coefficients of the reacting agents in the reaction mixture, the prediction of activity coefficients is required. This was done by means of ePC-SAFT which is presented in the following.

ePC-SAFT. To predict activity coefficients, the pure-component reference state was used in this work, indicated by the subscript 0*i*. Further, activity coefficients were predicted by using the respective fugacity coefficients φ_i as shown in eq 9. Note that γ_i is the mole fraction-based activity coefficient that can be transferred into the molality-based activity coefficient γ_i^m according to eq 10

$$\gamma_i = \frac{\varphi_i}{\varphi_{0i}} \quad (9)$$

$$a[-] = x_i\cdot\gamma_i = m_i\cdot\gamma_i^m \quad (10)$$

The required residual Helmholtz energy a^{res} to predict φ_i and φ_{0i} was calculated with ePC-SAFT.[27]

$$a^{res} = a^{hc} + a^{disp} + a^{assoc} + a^{ion} \quad (11)$$

The four free-energy contributions to calculate a^{res} are explained in the Supporting Information. To describe mixtures,[47,48] combining rules proposed by Berthelot and Lorentz[49,50] and Wolbach–Sandler[51] were applied in this work. These are combining rules for the mean segment diameter, mean dispersion-energy parameter and mean association-energy parameter. Only one binary interaction parameter k_{ij} was used in this work as shown in eq 14.

$$\sigma_{ij} = \frac{1}{2}\cdot(\sigma_i + \sigma_j) \quad (12)$$

$$\varepsilon^{A_iB_j} = \frac{1}{2}\cdot(\varepsilon^{A_iB_i} + \varepsilon^{A_jB_j}) \quad (13)$$

DOI: 10.1021/acsomega.8b03159
ACS Omega 2019, 4, 6264−6272

$$u_{ij} = \sqrt{u_i \cdot u_j} \cdot (1 - k_{ij}) \quad (14)$$

The ePC-SAFT pure-component and binary interaction parameters used in this work are listed in Tables 1 and 2.

Table 2. Overview of the ePC-SAFT Binary Interaction Parameters k_{ij} Used in This Work

binary pair	k_{ij} [−]
water−NADH[10]	−0.0585
water−NAD$^+$[10]	−0.0736
water−PEG[41c]	[a]
water−Na$^+$[56]	[b]
water−OH$^-$[56]	−0.25
Na$^+$−OH$^-$[56]	0.649

[a] $k_{ij}(T) = -0.135 + 0.0023439 \cdot (T[\mathrm{K}] - 298.15)$. [b] $k_{ij}(T) = 0.00046 - 0.007981 \cdot (T[\mathrm{K}] - 298.15)$. [c] Transposed digits in the original reference. Thus, value of the present work has to be used.

RESULTS AND DISCUSSION

Reaction Equilibrium. For the reaction equilibrium of the neat reactions and the validation with ePC-SAFT predictions the influence of 17 wt % PEG 6000 was studied with initial molalities of $m_{\mathrm{ketone},0} = m_{\mathrm{NADH},0} = 0.5$ mmol/kg$_{\mathrm{water}}$.

The results of the equilibrium measurements under neat conditions for the reduction of butanone and 2-pentanone are shown in Figure 2. The detailed mole fractions of each reacting agents at equilibrium are given in Tables S1 and S2 in the Supporting Information.

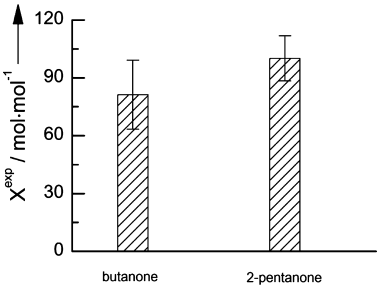

Figure 2. Experimental results for the reaction equilibrium expressed as X^{exp} under neat (cosolvent free) reaction conditions at 30 °C, 1 bar, and pH 7. Results for the reduction of butanone and 2-pentanone are shown for initial ketone molalities of 0.5 mmol/kg$_{\mathrm{water}}$ and for initial NADH molalities of 0.5 mmol/kg$_{\mathrm{water}}$, respectively. Detailed experimental data is given in Tables S1 and S2 in the Supporting Information.

As can be seen from Figure 2 for both reduction reactions, the reaction equilibrium position is located strongly on the side of the respective alcohol (butanol; 2-pentanol) as $X^{\mathrm{exp}} \gg 1$. Further, X^{exp}(2-pentanone reduction) = 100.1 ± 11.7 mol/mol is about 1.25 fold larger than X^{exp}(butanone reduction) = 81.2 ± 17.9 mol/mol. It is also visible that the uncertainty for X^{exp} is greater for the butanone reduction than for the 2-pentanone reduction, which is not unexpected because of the higher volatility of butanone over 2-pentanone. For both reduction reactions, the observed equilibrium composition X^{exp} was converted into the thermodynamic equilibrium constant K_{th} by using the ePC-SAFT predicted activity-coefficient ratios Γ. Predictions of Γ were based on the parameters from Tables 1 and 2. The predicted activity coefficients are listed in Table S3 in the Supporting Information. The predicted values for Γ and $K_{\mathrm{th}} \cdot a_{H^+}$ are given in Table 3. Note that the uncertainty in the experimental data was not transferred into the predicted value of $K_{\mathrm{th}} \cdot a_{H^+}$.

Table 3. Overview of the Experimentally Determined Reaction Equilibrium Position X^{exp}, the ePC-SAFT Predicted Activity Coefficient Ratio Γ with the Parameters from Tables 1 and 2, and the Resulting Value of $K_{\mathrm{th}} \cdot a_{H^+}$ for the Reduction of Butanone and 2-Pentanone at 30 °C, 1 bar, and pH 7 Catalyzed by ADH 270

ketone	X^{exp} [mol/mol]	Γ [mol/mol]	$K_{\mathrm{th}} \cdot a_{H^+}$ [−]
butanone	81.2 ± 17.9	4.071×10^{-2}	3.3
2-pentanone	100.1 ± 11.7	3.458×10^{-2}	3.5

The respective $K_{\mathrm{th}} \cdot a_{H^+}$ values were used to predict X^{exp} under the influence of 17 wt % of PEG 6000 based on eq 5. The results of the predictions and the validation with experimental data are given in Figure 3 and Table 4. A detailed list of all

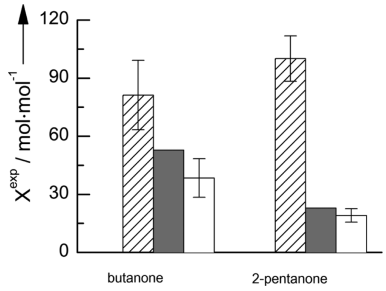

Figure 3. Comparison between the ePC-SAFT-predicted influence of 17 wt % of PEG 6000 on X^{exp} for the reduction of butanone and 2-pentanone, respectively (gray bars), and the experimentally determined values of X^{exp} under the influence of 17 wt % of PEG 6000 (white bars) at 30 °C, 1 bar, and pH 7. Striped bars represent the neat (cosolvent free) values used to determine $K_{\mathrm{th}} \cdot a_{H^+}$. ePC-SAFT predictions were based on the parameters listed in Tables 1 and 2.

Table 4. Comparison between the ePC-SAFT-Predicted Influence of 17 wt % of PEG 6000 on X^{pre} with the Experimentally Determined Values X^{exp} at 30 °C, 1 bar, and pH 7[a]

	neat conditions	17 wt %PEG 6000	
ketone	X^{exp} [mol/mol]	X^{pre} [mol/mol]	X^{exp} [mol/mol]
butanone	81.2 ± 17.9	52.9	38.4 ± 9.9
2-pentanone	100.1 ± 11.7	22.9	19.0 ± 3.4

[a] ePC-SAFT predictions of X^{pre} were based on the parameters listed in Tables 1 and 2.

mole fractions at equilibrium under 17 wt % of PEG 6000 for both reduction reactions is given in Tables S1 and S2 in the Supporting Information. Note that no experimental data of the reaction was used to fit any of the ePC-SAFT parameters and thus, the presented predictions are independent from any reaction data.

As can be clearly seen from Figure 3 and Table 4, ePC-SAFT is capable of predicting the cosolvent influence of 17 wt % PEG 6000 on X^{exp} of the reduction of butanone and 2-pentanone. For X^{exp} of the 2-pentanone reduction predictions are close to quantitatively correct within the experimental uncertainties. The higher deviation in the predictions for

DOI: 10.1021/acsomega.8b03159
ACS Omega 2019, 4, 6264−6272

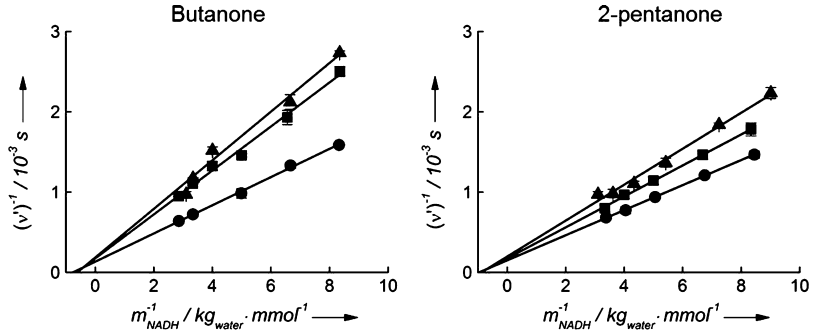

Figure 4. *Primary plots* for the determination of $K^{obs}_{M,ketone}$ and $K^{obs}_{M,NADH}$ under neat (cosolvent free) conditions for the reduction of butanone and 2-pentanone at 30 °C, 1 bar, and pH 7 catalyzed by ADH 270. Reciprocal normalized reaction rate $(\nu')^{-1}$ is plotted over the reciprocal initial molality of NADH m_{NADH}^{-1} for pseudo-constant molalities of butanone (triangles: 30 mmol/kg_{water}; squares: 50 mmol/kg_{water}; circles: 250 mmol/kg_{water}) in the left and pseudo-constant molalities of 2-pentanone (triangles: 30 mmol/kg_{water}; squares: 50 mmol/kg_{water}; circles: 100 mmol/kg_{water}) in the right diagram.[15]

butanone can be explained in the larger uncertainty in the experimental neat data used to determine $K_{th}\cdot a_{H^+}$.

These findings are discussed in the following. It might be expected that the ketones or alcohols are affected differently upon PEG addition. To investigate this, the ratio of activity coefficients of the reacting agents were analyzed. The activity coefficients of the reacting agents show that the ratio $\gamma_{butanone}(neat)/\gamma_{butanone}(PEG) = 2.3$ is very close to the ratio $\gamma_{2\text{-pentanone}}(neat)/\gamma_{2\text{-pentanone}}(PEG) = 2.4$. The same was observed for the activity-coefficient ratios of the respective alcohols butanol and 2-pentanol, and even for the substrate NADH. That is, PEG influences these activity-coefficient ratios very similarly, which in sum does not explain the reason behind the strong PEG influence on reaction equilibrium. In contrast, the ratio $\gamma_{NAD^+}(neat)/\gamma_{NAD^+}(PEG)$ for the reduction of butanone was predicted to be 0.039, whereas $\gamma_{NAD^+}(neat)/\gamma_{NAD^+}(PEG)$ for the reduction of 2-pentanone was predicted to be 0.065. This shows that the significantly higher PEG influence on 2-pentanone reduction is caused by the influence of PEG on the molecular interactions involving NAD^+. While this is an unexpected result, activity coefficients have been identified to be relevant even for reaction with isomers.[58] Thus, even for similar systems, a general cosolvent influence on reaction equilibria cannot be deduced.

To conclude, it was shown that X^{exp} for the reduction of butanone and 2-pentanone under neat conditions was similar within the experimental uncertainties, while the influence of 17 wt % of PEG 6000 was vastly different for both reactions. This proves that even for similar substrates that only differ by one methyl group ($-CH_2-$), assumptions of similar molecular interactions between the substrates and the cosolvent PEG 6000 might be very unreasonable, which showcases the need of a thermodynamic model to predict these interactions correctly and nonempirically. Because of the ability to account for the molecular interactions based on the residual Helmholtz energy predicted by ePC-SAFT, a quantification and prediction of the cosolvent effect of 17 wt % of PEG 6000 was possible for both reduction reactions. This further shows that thermodynamic activities lead to cosolvent independent constants, which should be chosen in future rather than falsely labeled molality-based "*constants*" which are not constant values at all.

Michaelis Constants. The influence of 17 wt % PEG 6000 on the kinetic parameters $K^{obs}_{M,ketone}$ and $K^{obs}_{M,NADH}$ was measured and predicted in this work. Figure 4 shows the *primary plots* for the reduction of butanone and 2-pentanone. The experimental results of $(\nu')^{-1}$ for each molality of the ketones and NADH are given in Tables S4 and S5 in the Supporting Information.

Figure 4 shows that the normalized reaction rate observed for the reduction of 2-pentanone is slightly higher than for the reduction of butanone for the same molalities of 30 and 50 mmol/kg_{water} of the ketones, respectively. Further, a linear relation between $(\nu')^{-1}$ and m_{NADH}^{-1} for each pseudo-constant molality of the respective ketone can be observed. The resulting *secondary plots* required for the determination of $K^{obs}_{M,ketone}$ and $K^{obs}_{M,NADH}$ are given in Figures S3 and S4 in the Supporting Information. Table 5 lists the experimentally determined Michaelis constants from the *secondary plots* under neat conditions for the ketone and NADH, respectively.

Table 5. Experimentally Determined Michaelis Constants for the Ketone $K^{obs}_{M,ketone}$ and NADH $K^{obs}_{M,NADH}$ for the Reduction of Butanone and 2-Pentaone under Neat Conditions at 30 °C, 1 bar, and pH 7 Catalyzed by ADH 270

ketone	$K^{obs}_{M,ketone}$ [mmol/kg_{water}]	$K^{obs}_{M,NADH}$ [mmol/kg_{water}]
butanone	14.0 ± 4.1	1.3 ± 0.1
2-pentanone[15]	15.8 ± 1.6	1.0 ± 0.1

It can be observed that K^{obs}_M values for the ketone and NADH are similar for both reactions. As observed also for X^{exp} under neat conditions, K^{obs}_M of butanone shows a larger uncertainty than for 2-pentanone, which can also be denoted to the higher volatility of butanone. It is noteworthy that the higher uncertainties arise from taking into account the uncertainties of each experimental data point in the *primary* and *secondary plots* by a Gaussian propagation of uncertainty (Taylor expansion) and not the R^2 of the fit lines. This leads to realistic experimental uncertainties in the determination of K^{obs}_M, highlighting the need of a predictive model to reduce experimental efforts and costs further.

As first step for predictions of K^{obs}_M, the activity-based Michaelis constants K^a_M were determined based on eq 8. The activity-based *primary plots* are given in Figure 5. Note that activity coefficient were predicted with the same ePC-SAFT parameters from Tables 1 and 2, as for the activity-coefficient predictions of $K_{th}\cdot a_{H^+}$.

As can be clearly seen from Figure 5, the kinetic information of the reactions are preserved from the molality-based *primary plots* given in Figure 4. These include the increased reaction

DOI: 10.1021/acsomega.8b03159
ACS Omega 2019, 4, 6264−6272

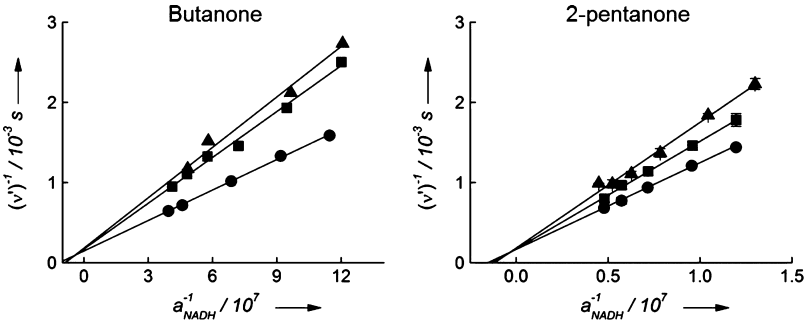

Figure 5. *Primary plots* for the determination of $K^{a}_{M,ketone}$ and $K^{a}_{M,NADH}$ under neat (cosolvent free) conditions for the reduction of butanone and 2-pentanone at 30 °C, 1 bar, and pH 7 catalyzed by ADH 270. Reciprocal normalized reaction rate $(\nu')^{-1}$ plotted over the reciprocal initial activity of NADH $a_{NADH}{}^{-1}$ for pseudo-constant molalities of butanone (triangles: 30 mmol/kg_{water}; squares: 50 mmol/kg_{water}; circles: 250 mmol/kg_{water}) in the left diagram and for pseudo-constant molalities of 2-pentanone (triangles: 30 mmol/kg_{water}; squares: 50 mmol/kg_{water}; circles: 100 mmol/kg_{water}) in the right diagram.[15]

rate for increased molalities of the ketone, the linear relation required to obtain the *secondary plots*, and the intersects of the fit lines in the second quadrant of the diagram. The activity coefficients predicted to obtain the activities of NADH and the resulting *secondary plots* are given in Tables S8 and S9, Figures S5 and S6 in the Supporting Information. Predicted values for K^{a}_{M} and $K^{a}_{i,NADH}$ required for the predictions of K^{obs}_{M} under the influence of 17 wt % of PEG 6000 are listed in Table 6.

Table 6. Determined Activity-Based Michaelis Constants K^{a}_{M} and Inhibition Constant K^{a}_{i} for the Reduction of Butanone and 2-Pentanone at 30 °C, 1 bar, and pH 7 Catalyzed by ADH 270[a]

ketone	$K^{a}_{M,ketone}$ [−]	$K^{a}_{M,NADH}$ [−]	$K^{a}_{i,NADH}$ [−]
butanone	0.08	8.35×10^{-8}	2.39×10^{-7}
2-pentanone[15]	0.30	5.40×10^{-8}	2.78×10^{-7}

[a]Required activity coefficients were predicted with ePC-SAFT with parameters from Tables 1 and 2.

While K^{obs}_{M} are mostly equal for both reactions, K^{a}_{M} values especially of the ketones differ significantly from each other for both reactions. This is caused by the nonideality of the reaction mixtures, which is different because of the different ketones present in the respective reaction. As can be seen from Tables S8 and S9 in the Supporting Information, activity coefficients of NADH are similar for both reactions. This is not the case for the activity coefficients of butanone and 2-pentanone (Table S10 in the Supporting Information). Activity coefficients of butanone are vastly different from being unity ($\gamma_{butanone} \neq 1$), whereas activity coefficients of 2-pentanone are much closer to unity. This shows that the reaction mixtures containing butanone are stronger nonideal than the reaction mixtures containing 2-pentanone. The determined activity-based Michaelis constants (Table 7) were used to predict the influence of 17 wt % of PEG 6000 on K^{obs}_{M}. The results of the predictions and a comparison to experimental data are given in Figure 6 and Table 7.

Figure 6 and Table 7 show that ePC-SAFT predicts a decrease for $K^{obs}_{M,ketone}$ and $K^{obs}_{M,NADH}$ for the reduction of butanone and 2-pentanone under the influence of 17 wt % PEG 6000 compared with their neat reaction mixtures. While the decrease of $K^{obs}_{M,NADH}$ is predicted to be mostly equal for both reactions, the decrease of $K^{obs}_{M,butanone}$ is predicted to be twofold larger than that of $K^{obs}_{M,2\text{-}pentanone}$, thus showing that the influence of 17 wt % PEG 6000 is not equal for both reactions. Comparing the ePC-SAFT predictions with experimental data for the reactions under 17 wt % PEG 6000 influence (*primary* and *secondary plots* including the detailed values given in Tables S12 to S15 and Figures S7 to S9 in the Supporting Information) shows an at least qualitative agreement between K^{pre}_{M} and K^{obs}_{M} for the reduction of butanone and qualitative to quantitative predictions for the reduction of 2-pentanone.

To conclude, experimental Michaelis constants K^{obs}_{M} for the reduction of butanone and 2-pentanone under neat conditions were similar within the experimental uncertainties. Interestingly, the same was observed also for the reaction equilibrium of both reaction under neat conditions. However, the influence of 17 wt % of PEG 6000 on K^{obs}_{M} was unexpected: While $K^{obs}_{M,NADH}$ was decreased by a factor of two for both reduction reactions under cosolvent, $K^{obs}_{M,ketone}$ was decreased differently strong for both reactions. These findings show that both Michaelis constant are not necessarily influenced in the same way when a cosolvent is present. This cosolvent effect on K^{obs}_{M}, caused by different molecular interactions for both reduction reactions, was successfully predicted with ePC-SAFT in the form of the respective activity coefficients of the ketone and NADH under neat conditions and under the influence of 17 wt

Table 7. Comparison between the ePC-SAFT Predicted Michaelis Constants $K^{pre}_{M,ketone}$ and $K^{pre}_{M,NADH}$ for the Reduction of Butanone and 2-Pentanone under the Influence of 17 wt % of PEG 6000 at 30 °C, 1 bar, and pH 7 Catalyzed by ADH 270[a]

	neat	17 wt %PEG 6000		neat	17 wt %PEG 6000	
letone	$K^{obs}_{M,ketone}$ [mmol/kg_{water}]	$K^{pre}_{M,ketone}$ [mmol/kg_{water}]	$K^{obs}_{M,ketone}$ [mmol/kg_{water}]	$K^{obs}_{M,NADH}$ [mmol/kg_{water}]	$K^{pre}_{M,NADH}$ [mmol/kg_{water}]	$K^{obs}_{M,NADH}$ [mmol/kg_{water}]
butanone	14.0 ± 4.1	2.8	4.0 ± 0.4	1.3 ± 0.1	0.7	0.5 ± 0.1
2-pentanone[15]	15.8 ± 1.6	6.2	6.9 ± 0.4	1.0 ± 0.9	0.5	0.5 ± 0.1

[a]Reference values of the neat reaction are also provided. Activity coefficients required for the predictions were estimated with ePC-SAFT based on the parameters from Tables 1 and 2.

DOI: 10.1021/acsomega.8b03159
ACS Omega 2019, 4, 6264−6272

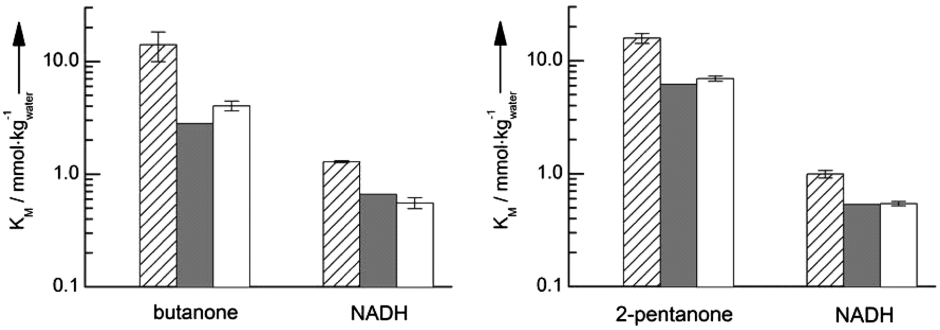

Figure 6. Comparison between the observed Michaelis constants K_M^{obs} for neat reaction conditions (white bars) and under the influence of 17 wt % PEG 6000 (striped bars) for the reduction of butanone (left diagram) and 2-pentanone[15] (right diagram) catalyzed by ADH 270 at 30 °C, 1 bar, and pH 7. Gray bars represent the ePC-SAFT prediction of the respective K_M^{obs} based on the determined activity-based K_M^a and $K_{i,NADH}^a$ given in Table 7. Activity coefficients required for the predictions were estimated with ePC-SAFT based on the parameters from Tables 1 and 2.

% of PEG 6000. Additionally, this approach proves that the enzyme−cosolvent interactions play a minor role in the change of K_M^{obs} under cosolvent influence. In sum, the use of PEG was found to be very meaningful as the kinetics of both reactions could be improved strongly, as all Michaelis constants were significantly reduced upon PEG addition.

CONCLUSION

To conclude, this work aimed at providing the base for a thermodynamic activity-based framework that might enable the prediction of cosolvent influences on reaction equilibria and Michaelis constants of enzyme-catalyzed reactions. This framework accounts for cosolvent effects on the interactions among reacting agents and between reacting agents and solvent, which seem to be the key for predicting reaction equilibria under cosolvent influence. Further, the framework accounts for cosolvent-induced interactions between solvent and substrate. In contrast, enzyme interactions are not taken into account for predicting Michaelis constants and reaction equilibria.

This work feeds the thermodynamic activity-based approach by ePC-SAFT predicted activity coefficients of the reacting agents under cosolvent influence. The approach was applied to successfully predict the influence of 17 wt % of PEG 6000 on reaction equilibria and Michaelis constants of the reductions of butanone and 2-pentanone catalyzed by the enzyme ADH 270. The quality of the predictions means a significant improvement over other literature works which describe cosolvent effects empirically. It further shows that enzyme-independent substrate−cosolvent interactions are the major driving force for the cosolvent induced changes in the Michaelis constants. This is expressed by the activity coefficients of the substrates upon PEG addition. Additionally, these findings indicate that cosolvent−enzyme interactions might play a minor role compared with substrate−cosolvent interactions. These findings support hypotheses from our previous publications and enlarge the applicability range of the developed activity-based approach.

The quality of the simultaneous predictions of reaction equilibria and Michaelis constants points to the importance to account for thermodynamic activities to understand and quantify cosolvent effects on reaction equilibrium and Michaelis constants of enzymatic reactions. This approach provides a framework that might enable the screening of cosolvents a priori to avoid time-consuming and costly experiments and allows next steps toward predictions of enzymatic reactions in cellulo.

MATERIALS AND METHODS

Chemicals. In this work, HEPES and PEG 6000 were purchased from VWR International. 2-Pentanone and β-nicotinamide adenine dinucleotide disodium salt ($NADHNa_2$) were obtained from Sigma-Aldrich. Sodium hydroxide (NaOH) and butanone were purchased from Alfa Aesar. The genetically modified alcohol dehydrogenase (ADH 270) was obtained from evoxx technologies. All chemicals were used without further purification and all samples were prepared using Millipore water from the Milli-Q provided by Merck Millipore. An overview of all chemicals used in this work is given in Table S16 in the Supporting Information.

Kinetic and Equilibrium Measurements. Kinetic and equilibrium measurements were carried out in 0.1 mol/kg$_{water}$ HEPES buffer adjusted to a pH of 7 with sodium hydroxide at temperature T = 303.15 K and p = 1 bar. The pH of the buffer and each sample was measured with a pH electrode from Mettler Toledo (uncertainty ± 0.01).

In this work, 17 wt % of PEG 6000 was added to the buffer to mimic the cosolvent. The stability and activity of ADH 270 in the buffer and under the influence of PEG 6000 was proven in a previous work.[15] In the first step for the kinetic measurements, the stock solutions of the respective ketone (butanone; 2-pentanone) were prepared in equal number to the NADH molalities measured. The ketone was added gravimetrically to an Eppendorf cup on a XS analytical scale provided by Mettler Toledo (uncertainty ± 0.01 mg) and mixed with buffer afterward. The Eppendorf cups were filled to the maximum capacity to decrease the vapor phase, minimizing losses of ketone during the short storage time before experiments. The ketone stock solutions were preheated after preparation in an Eppendorf ThermoMixer C at 30 °C. Butanone molalities of the neat reaction investigated were 30, 50, and 250 mmol/kg$_{water}$ and 30, 50, and 100 mmol/kg$_{water}$ for the PEG 6000 measurements. 2-Pentanone molalities investigated were 30, 50, and 100 mmol/kg$_{water}$ for neat and PEG 6000 measurements. Afterward, NADH was added gravimetrically to the ketone solution. A NADH stock solution was not used because of known instability of NADH in solution.[57] Thus, NADH solutions were freshly prepared with NADH molalities of 0.1, 0.15, 0.2, 0.25, 0.3, and 0.35 mmol/kg$_{water}$. The enzyme stock solution was prepared by gravimetrically adding 1 wt % of enzyme to 2 mL of buffer and storage of the

DOI: 10.1021/acsomega.8b03159
ACS Omega 2019, 4, 6264−6272

Eppendorf cup on ice. To initiate the kinetic measurements 20 mg of the enzyme solution were transferred into a quartz cuvette supRAsil TYP 114-QS from Hellma Analytics which was preheated to 30 °C in an Eppendorf BioSpectrometer and direct addition of 1 g substrate solution containing the respective ketone (butanone or 2-pentanone) and NADH. The extinction measurement over time was carried out at 340 nm wavelength (extinction maxima of NADH). The respective calibration curves and extinction coefficients of NADH in the buffer and in buffer + 17 wt % PEG 6000 are given in Figure S1 the Supporting Information.

For reaction equilibrium measurements sample preparation was identical to the kinetic measurements with the only difference in the considered molalities. For the reduction of butanone and 2-pentanone under neat and 17 wt % of PEG 6000 influence equimolar concentrations of the ketone and NADH were used. This was done to ensure the determination of equilibrium position with lowest experimental uncertainty (uncertainty increases by using much lower substrate molalities). Molalities of NADH and the respective ketone (butanone or 2-pentanone) were chosen to be 0.5 mmol/kg_{water}. Measurements of the reaction equilibrium were performed by extinction over time measurements until the extinction did not change ($dE/dt = 0$). Equilibrium position was then verified by addition of the substrate solution (ketone and NADH) to check if the enzyme was still active and not denatured (shown in Figure S2 in the Supporting Information). Data reduction of the equilibrium measurements was done based on a mole balance as shown in eq 15.

$$X^{exp} = \frac{(n_{NADH,0} - n_{NADH})^2}{(n_{ketone,0} - n_{NADH})\cdot(n_{NADH,0} - n_{NADH})} \quad (15)$$

■ ASSOCIATED CONTENT

Supporting Information

The Supporting Information is available free of charge on the ACS Publications website at DOI: 10.1021/acsomega.8b03159.

All experimentally determined raw data and a listing of all activity coefficients predicted in this work and further, diagrams not seen suitable for the main text are provided (PDF)

■ AUTHOR INFORMATION

Corresponding Author

*E-mail: christoph.held@tu-dortmund.de (C.H.).

ORCID

Gabriele Sadowski: 0000-0002-5038-9152

Christoph Held: 0000-0003-1074-177X

Author Contributions

The manuscript was written by A.W. and C.H. All authors have given approval to the final version of the manuscript and declare no conflict of interest.

Notes

The authors declare no competing financial interest.

■ ACKNOWLEDGMENTS

A.W. and C.H. gratefully acknowledge the financial support by the Cluster of Excellence RESOLV (EXC 1069) funded by the Deutsche Forschungsgemeinschaft (DFG).

■ ABBREVIATIONS

ACP	acetophenone
ADH 270	alcohol dehydrogenase 270
ATPS	aqueous two phase separation systems
COSMO	conductor-like screening model
eNRTL	electrolyte nonrandom two-liquid (eNRTL) model
ePC-SAFT	electrolyte perturbed-chain statistical associating fluid theory
HEPES	4-(2-hydroxyethyl)-1-piperazineethanesulfonic acid
NAD^+	nicotinamide adenine dinucleotide in its deprotonated form
NADH	nicotinamide adenine dinucleotide in its protonated form
NaOH	sodium hydroxide
PEG 6000	polyethylene glycol 6000
SI	Supporting Information
VWR	VWR International

■ REFERENCES

(1) Straathof, A. J. J.; Panke, S.; Schmid, A. The production of fine chemicals by biotransformations. *Curr. Opin. Biotechnol.* **2002**, *13*, 548−556.

(2) Fessner, W.-D.; Anthonsen, T. *Modern Biocatalysis: Stereoselective and Environmentally Friendly Reactions*; John Wiley & Sons, 2009.

(3) Schulze, B.; Wubbolts, M. G. Biocatalysis for industrial production of fine chemicals. *Curr. Opin. Biotechnol.* **1999**, *10*, 609−615.

(4) Carrea, G.; Riva, S. Properties and synthetic applications of enzymes in organic solvents. *Angew. Chem., Int. Ed.* **2000**, *39*, 2226−2254.

(5) Bolm, C.; Beckmann, O.; Dabard, O. A. G. The Search for New Environmentally Friendly Chemical Processes. *Angew. Chem., Int. Ed.* **1999**, *38*, 907−909.

(6) Hansen, C. A.; Frost, J. W. Deoxygenation of Polyhydroxybenzenes: An Alternative Strategy for the Benzene-Free Synthesis of Aromatic Chemicals. *J. Am. Chem. Soc.* **2002**, *124*, 5926−5927.

(7) Bisswanger, H. *Enzymkinetik: Theorie und Methoden, 3. Auflage*; Wiley Online Library, 2000.

(8) Segel, I. H. *Enzyme Kinetics: Behavior and Analysis of Rapid Equilibrium and Steady State Enzyme Systems*; Wiley: New York, 1975.

(9) Atkinson, D. E. Limitation of Metabolite Concentrations and the Conservation of Solvent Capacity in the Living Cell. In *Current Topics in Cellular Regulation*; Horecker, B. L., Stadtman, E. R., Eds.; Academic Press, 1969; Vol. *1*, pp 29−43.

(10) Wangler, A.; Loll, R.; Greinert, T.; Sadowski, G.; Held, C. Predicting the high concentration co-solvent influence on the reaction equilibria of the ADH-catalyzed reduction of acetophenone. *J. Chem. Thermodyn.* **2019**, *128*, 275−282.

(11) Wangler, A.; Canales, R.; Held, C.; Luong, T. Q.; Winter, R.; Zaitsau, D. H.; Verevkin, S. P.; Sadowski, G. Co-solvent effects on reaction rate and reaction equilibrium of an enzymatic peptide hydrolysis. *Phys. Chem. Chem. Phys.* **2018**, *20*, 11317−11326.

(12) Wangler, A.; Schmidt, C.; Sadowski, G.; Held, C. Standard Gibbs Energy of Metabolic Reactions: III The 3-Phosphoglycerate Kinase Reaction. *ACS Omega* **2018**, *3*, 1783−1790.

(13) Voges, M.; Fischer, F.; Neuhaus, M.; Sadowski, G.; Held, C. Measuring and Predicting Thermodynamic Limitation of an Alcohol Dehydrogenase Reaction. *Ind. Eng. Chem. Res.* **2017**, *56*, 5535−5546.

(14) Voges, M.; Schmidt, F.; Wolff, D.; Sadowski, G.; Held, C. Thermodynamics of the alanine aminotransferase reaction. *Fluid Phase Equilib.* **2016**, *422*, 87−98.

(15) Wangler, A.; Böttcher, D.; Hüser, A.; Sadowski, G.; Held, C. Prediction and Experimental Validation of Co-Solvent Influence on

DOI: 10.1021/acsomega.8b03159
ACS Omega 2019, 4, 6264−6272

Michaelis Constants: A Thermodynamic Activity-Based Approach. *Chem.—Eur. J.* **2018**, *24*, 16418−16425.
(16) Wangler, A.; Bunse, M.-J.; Sadowski, G.; Held, C. Thermodynamic Activity-based Michaelis constants. *Kinetics of Enzymatic Synthesis*; IntechOpen, 2018.
(17) Brooks, C. L.; Karplus, M. Solvent effects on protein motion and protein effects on solvent motion. *J. Mol. Biol.* **1989**, *208*, 159−181.
(18) Kragl, U.; Eckstein, M.; Kaftzik, N. Enzyme catalysis in ionic liquids. *Curr. Opin. Biotechnol.* **2002**, *13*, 565−571.
(19) MacKerell, A. D.; Nilsson, L.; Rigler, R.; Saenger, W. Molecular dynamics simulations of ribonuclease T1: analysis of the effect of solvent on the structure, fluctuations, and active site of the free enzyme. *Biochemistry* **1988**, *27*, 4547−4556.
(20) Pleiss, J. Thermodynamic Activity-Based Interpretation of Enzyme Kinetics. *Trends Biotechnol.* **2017**, *35*, 379−382.
(21) Grosch, J.-H.; Wagner, D.; Nistelkas, V.; Spieß, A. C. Thermodynamic activity-based intrinsic enzyme kinetic sheds light on enzyme-solvent interactions. *Biotechnol. Prog.* **2016**, *33*, 96−103.
(22) Altuntepe, E.; Emel'yanenko, V. N.; Forster-Rotgers, M.; Sadowski, G.; Verevkin, S. P.; Held, C. Thermodynamics of enzyme-catalyzed esterifications: II. Levulinic acid esterification with short-chain alcohols. *Appl. Microbiol. Biotechnol.* **2017**, *101*, 7509−7521.
(23) Song, Y.; Chen, C.-C. Symmetric Electrolyte Nonrandom Two-Liquid Activity Coefficient Model. *Ind. Eng. Chem. Res.* **2009**, *48*, 7788−7797.
(24) Sander, B.; Fredenslund, A.; Rasmussen, P. Calculation of vapour-liquid equilibria in mixed solvent/salt systems using an extended UNIQUAC equation. *Chem. Eng. Sci.* **1986**, *41*, 1171−1183.
(25) Pitzer, K. S. Thermodynamics of electrolytes. I. Theoretical basis and general equations. *J. Phys. Chem.* **1973**, *77*, 268−277.
(26) Klamt, A.; Schüürmann, G. COSMO: a new approach to dielectric screening in solvents with explicit expressions for the screening energy and its gradient. *J. Chem. Soc., Perkin Trans. 2* **1993**, 799−805.
(27) Cameretti, L. F.; Sadowski, G.; Mollerup, J. M. Modeling of Aqueous Electrolyte Solutions with Perturbed-Chain Statistical Associated Fluid Theory. *Ind. Eng. Chem. Res.* **2005**, *44*, 3355−3362.
(28) Gross, J.; Sadowski, G. Modeling Polymer Systems Using the Perturbed-Chain Statistical Associating Fluid Theory Equation of State. *Ind. Eng. Chem. Res.* **2002**, *41*, 1084−1093.
(29) Meurer, F.; Bobrownik, M.; Sadowski, G.; Held, C. Standard Gibbs Energy of Metabolic Reactions: I. Hexokinase Reaction. *Biochemistry* **2016**, *55*, 5665−5674.
(30) Altuntepe, E.; Greinert, T.; Hartmann, F.; Reinhardt, A.; Sadowski, G.; Held, C. Thermodynamics of enzyme-catalyzed esterifications: I. Succinic acid esterification with ethanol. *Appl. Microbiol. Biotechnol.* **2017**, *101*, 5973−5984.
(31) Goldberg, R. N.; Tewari, Y. B.; Bell, D.; Fazio, K.; Anderson, E. Thermodynamics of Enzyme-Catalyzed Reactions: Part 1. Oxidoreductases. *J. Phys. Chem. Ref. Data* **1993**, *22*, 515−582.
(32) Cooper, G. M.; Hausman, R. E. *The Cell: A Molecular Approach*; ASM Press, 2009.
(33) DeSantis, G.; Jones, J. B. Chemical modification of enzymes for enhanced functionality. *Curr. Opin. Biotechnol.* **1999**, *10*, 324−330.
(34) Börjesson, J.; Peterson, R.; Tjerneld, F. Enhanced enzymatic conversion of softwood lignocellulose by poly(ethylene glycol) addition. *Enzyme Microb. Technol.* **2007**, *40*, 754−762.
(35) Beckman, J. S.; Minor, R. L.; White, C. W.; Repine, J. E.; Rosen, G. M.; Freeman, B. A. Superoxide dismutase and catalase conjugated to polyethylene glycol increases endothelial enzyme activity and oxidant resistance. *J. Biol. Chem.* **1988**, *263*, 6884−6892.
(36) Uma Maheswar Rao, J. L.; Satyanarayana, T. Enhanced secretion and low temperature stabilization of a hyperthermostable and Ca2+-independent α-amylase of Geobacillus thermoleovorans by surfactants. *Lett. Appl. Microbiol.* **2003**, *36*, 191−196.
(37) Chen, J.; Spear, S. K.; Huddleston, J. G.; Rogers, R. D. Polyethylene glycol and solutions of polyethylene glycol as green reaction media. *Green Chem.* **2005**, *7*, 64−82.
(38) Kwon, S. J.; Han, J. J.; Rhee, J. S. Production and in situ separation of mono- or diacylglycerol catalyzed by lipases in n-hexane. *Enzyme Microb. Technol.* **1995**, *17*, 700−704.
(39) Wysoczanska, K.; Macedo, E. A. Effect of molecular weight of polyethylene glycol on the partitioning of DNP-amino acids: PEG (4000, 6000) with sodium citrate at 298.15 K. *Fluid Phase Equilib.* **2016**, *428*, 84−91.
(40) Wysoczanska, K.; Silvério, S. C.; Teixeira, J. A.; Macedo, E. A. Cation effect on the (PEG 8000 + sodium sulfate) and (PEG 8000 + magnesium sulfate) aqueous two-phase system: Relative hydrophobicity of the equilibrium phases. *J. Chem. Thermodyn.* **2015**, *91*, 321−326.
(41) Reschke, T.; Brandenbusch, C.; Sadowski, G. Modeling aqueous two-phase systems: I. Polyethylene glycol and inorganic salts as ATPS former. *Fluid Phase Equilib.* **2014**, *368*, 91−103.
(42) Chen, J.-P.; Lee, M.-S. Enhanced production of Serratia marcescens chitinase in PEG/dextran aqueous two-phase systems. *Enzyme Microb. Technol.* **1995**, *17*, 1021−1027.
(43) Gao, M.; Estel, K.; Seeliger, J.; Friedrich, R. P.; Dogan, S.; Wanker, E. E.; Winter, R.; Ebbinghaus, S. Modulation of human IAPP fibrillation: cosolutes, crowders and chaperones. *Phys. Chem. Chem. Phys.* **2015**, *17*, 8338−8348.
(44) Gnutt, D.; Gao, M.; Brylski, O.; Heyden, M.; Ebbinghaus, S. Excluded-Volume Effects in Living Cells. *Angew. Chem., Int. Ed.* **2014**, *54*, 2548−2551.
(45) Kuby, S. A. *A Study of Enzymes*; CRC Press, 1990; Vol. *2*.
(46) Pleiss, J. Thermodynamic Activity-Based Progress Curve Analysis in Enzyme Kinetics. *Trends Biotechnol.* **2018**, *36*, 234−238.
(47) Held, C.; Reschke, T.; Müller, R.; Kunz, W.; Sadowski, G. Measuring and modeling aqueous electrolyte/amino-acid solutions with ePC-SAFT. *J. Chem. Thermodyn.* **2014**, *68*, 1−12.
(48) Nann, A.; Held, C.; Sadowski, G. Liquid-Liquid Equilibria of 1-Butanol/Water/IL Systems. *Ind. Eng. Chem. Res.* **2013**, *52*, 18472−18481.
(49) Berthelot, D. Sur le mélange des gaz. *C. R. Hebd. Séances Acad. Sci.* **1898**, *126*, 1703−1855.
(50) Lorentz, H. A. Ueber die Anwendung des Satzes vom Virial in der kinetischen Theorie der Gase. *Ann. Phys.* **1881**, *248*, 127−136.
(51) Wolbach, J. P.; Sandler, S. I. Using Molecular Orbital Calculations To Describe the Phase Behavior of Cross-associating Mixtures. *Ind. Eng. Chem. Res.* **1998**, *37*, 2917−2928.
(52) Fuchs, D.; Fischer, J.; Tumakaka, F.; Sadowski, G. Solubility of Amino Acids: Influence of the pH value and the Addition of Alcoholic Cosolvents on Aqueous Solubility. *Ind. Eng. Chem. Res.* **2006**, *45*, 6578−6584.
(53) Kleiner, M.; Gross, J. An equation of state contribution for polar components: Polarizable dipoles. *AIChE J.* **2006**, *52*, 1951−1961.
(54) Zarei, S.; Feyzi, F. Boyle temperature from SAFT, PC-SAFT and SAFT-VR equations of state. *J. Mol. Liq.* **2013**, *187*, 114−128.
(55) Grenner, A.; Kontogeorgis, G. M.; von Solms, N.; Michelsen, M. L. Modeling phase equilibria of alkanols with the simplified PC-SAFT equation of state and generalized pure compound parameters. *Fluid Phase Equilib.* **2007**, *258*, 83−94.
(56) Held, C.; Reschke, T.; Mohammad, S.; Luza, A.; Sadowski, G. ePC-SAFT revised. *Chem. Eng. Res. Des.* **2014**, *92*, 2884−2897.
(57) Gallati, H. Stabilisierung des reduzierten β-Nicotinamid-Adenin-Dinucleotid in einem organischen Lösungsmittel. *Clin. Chem. Lab. Med.* **1976**, *14*, 9−14.
(58) Hoffmann, P.; Held, C.; Maskow, T.; Sadowski, G. A thermodynamic investigation of the glucose-6-phosphate isomerization. *Biophys. Chem.* **2014**, *195*, 22−31.

DOI: 10.1021/acsomega.8b03159
ACS Omega 2019, 4, 6264−6272